Chaotic Modeling and Simulation (CMSIM) 2: 167–176, 2016

The Spectral Chaos in a Spherically Centered Layered Dielectric Cavity Resonator

Zoya E. Eremenko, Ekaterina S. Kuznetsova, Luka D. Shostenko, Yuriy V. Tarasov, and Igor N. Volovichev

O. Ya. Usikov Institute for Radiophysics and Electronics of National Academy of Sciences of Ukraine, Kharkov, Ukraine
(E-mail:zoya.eremenko@gmail.com)

Abstract. This paper deals with the study of chaotic spectral wave properties of a cavity sphere layered central-symmetric dielectric resonator. The analytical and numerical research was carried out. It is determined that resonant frequencies of a given layered resonator accurately coincide with the resonant frequencies of inhomogeneous resonator with specified oscillation indices if the radius of inner sphere is much less than the outer resonator radius. Increasing the radius of inner sphere these resonant frequencies shift to smaller values and new additional resonances appear, which cannot be identified by the same oscillation indices and it can be considered as possible chaotic presentation. The probability of inter-frequency interval distribution has signs of spectral chaos in studied structure.
Keywords: Sphere dielectric central-symmetric resonator, spectral wave properties, resonant frequencies, oscillation indices, signs of spectral chaos, probability of inter-frequency interval distribution.

1 Introduction

Our aim is to study the chaotic properties of a layered spherical dielectric cavity resonator with a inner centered spherical dielectric sphere. Dielectric resonators are known to be widely used in optics, laser technology, solid-state electronics (see, for example, Refs. [1,2]). The change of the oscillation spectrum of such resonators strongly depends on both inhomogeneities in the dielectric filling and the resonator shape. For practical applications it is extremely important to know the degree of regularity or randomness of the frequency spectrum. The detailed analysis of the spectrum chaotic properties for different resonant systems can be found, for instance, in [3].

The resonators with electromagnetic wave oscillations are often similar to classical dynamic billiards. Spectral properties of classical dynamical billiards have been thoroughly studied to date (see, e. g., the book [4]). The spectral properties of wave billiard systems are the subject of study by the relatively young field of physics, called “quantum (or wave) chaos” [5,6]. Using the

Received: 21 March 2015 / Accepted: 10 February 2016

ISSN 2241-0503

terminology given in paper [7], such systems can be called composite billiards. It is necessary to underline that the presence of additional spatial scale in wave billiards — the wavelength λ — results in serious limitations when trying to describe the chaotic properties of their spectra using the ray approach. In particular, there exist the ray splitting on the interface of different edges in the composite billiards [8,9], which cannot be captured by the classical dynamics. Thus, the ray approach is not well-suited to wave billiard-type systems, so their chaotic properties have to be studied, in general, applying of wave equations.

Statistic analysis of the wave system spectrum is mainly based on the methods used in the classical chaos dynamics, for instance, on the study of inter-frequency interval distribution, spectral rigidity and so on [5,6,10]. The goal of the present work is to investigate spectral properties of layered cavity resonators starting from electromagnetic wave approach. To reach this objective we apply the calculation technique consisting of rigorous splitting of oscillation modes by means of the operational method. This technique was used previously for inhomogeneous waveguides and resonators with bulk and surface inhomogeneities [11–14]. The result of the mode splitting in such complicate and conventionally non-integrable systems is the appearance of specific potentials of operator nature in the wave equation. The structure of these potentials gives rise to the possibility of studying the oscillation spectrum both numerically and analytically.

The spectrum of spherical resonator with homogeneous dielectric inside is strongly degenerate due to the central symmetry. The degeneracy leads to the clustering of the probability distribution maximum for inter-frequency intervals near zero value. It is quite natural to expect that when the spherical resonator becomes layered due to the spherical inner dielectric the spectrum degeneracy is removed. This is strongly expected to be so at least in the case of the symmetry violation.

In the present work we attempt to answer the following questions. What is the type of the probability distribution for inter-frequency intervals in the case of composite (layered) spherical resonator with and without the spatial symmetry? What is the qualitative nature of deformation of the probability distribution when spatial symmetry is violated? What are the signatures of classical chaos in this distribution?

2 Problem statement and basic relationships

We are interested in eigen-oscillations of an electromagnetic resonator taken in the form of ideal conducting sphere of radius $R_{\rm out}$ filled with homogeneous dielectric of permittivity $\varepsilon_{\rm out}$, in which a centered inner dielectric sphere of smaller radius $R_{\rm in}$ is placed, whose permittivity is $\varepsilon_{\rm in}$ (see Fig. 1).

The electromagnetic field inside the resonator can be expressed through electrical and magnetic Hertz functions, $U(\mathbf{r})$ and $V(\mathbf{r})$ [15]. Using these functions, we can go over to Debye potentials $\Psi_{U,V}(\mathbf{r})$ $\Psi_U(\mathbf{r}) = r^{-1}U(\mathbf{r})$ and

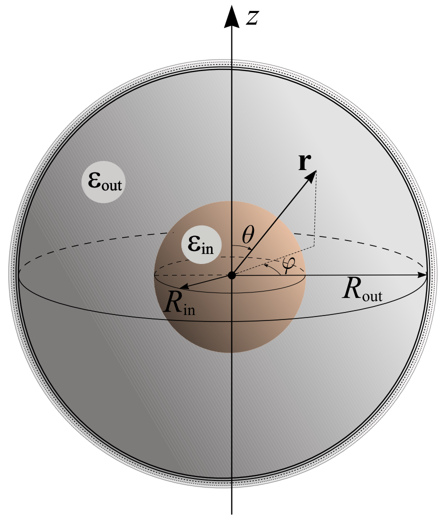

Fig. 1. Composite double-spherical dielectric cavity resonator.

$\Psi_V(\mathbf{r}) = r^{-1}V(\mathbf{r})$ [15,16] both obeying the same Helmholtz equation,

$$\left[\Delta + k^2\varepsilon(\mathbf{r})\right]\Psi(\mathbf{r}) = \frac{1}{r^2}\frac{\partial}{\partial r}\left(r^2\frac{\partial\Psi}{\partial r}\right) + \frac{1}{r^2\sin\vartheta}\frac{\partial}{\partial\vartheta}\left(\sin\theta\frac{\partial\Psi}{\partial\vartheta}\right) + \frac{1}{r^2\sin^2\theta}\frac{\partial^2\Psi}{\partial\varphi^2} + k^2\varepsilon(\mathbf{r})\Psi = 0 \tag{1}$$

(ϑ and φ are polar and azimuthal angle variables), but different independent boundary conditions,

$$\frac{\partial}{\partial r}\left(r\Psi_U\right)\bigg|_{r=R_{\text{out}}} = 0 \ , \tag{2a}$$

$$\Psi_V\bigg|_{r=R_{\text{out}}} = 0 \ . \tag{2b}$$

The first condition belongs to the class of so-called Robin's boundary conditions (see, e. g., Ref. [17]), the second one is the well-known Dirichlet condition. The conditions (2) for the electrical and magnetic Debye potentials allows to find these potentials independently from each other, which may be interpreted as the possibility to separate electrical and magnetic-type oscillation in the inhomogeneous spherical resonator.

We will consider the resonator inhomogeneity according to quantum-mechanical perturbation approach. If we take the inhomogeneity as a potential in Schrodinger equation we can write the permittivity in the equation (1) as a "weighted" sum of permittivities of inner and outer dielectric spheres,

$$\varepsilon(\mathbf{r}) = \varepsilon_{\text{in}}\boldsymbol{\Theta}\big(\mathbf{r}\in\Omega_{\text{in}}\big) + \varepsilon_{\text{out}}\boldsymbol{\Theta}\big(\mathbf{r}\in\Omega_{\text{out}}\setminus\Omega_{\text{in}}\big) \ . \tag{3}$$

Here $\boldsymbol{\Theta}(A)$ stands for the logical theta-function determined as

$$\boldsymbol{\Theta}(A)=\begin{cases}1\ , & \text{if } A=\text{true}\\ 0\ , & \text{if } A=\text{false}\end{cases}\ , \tag{4}$$

Ω_{in} and Ω_{out} are the portions of spatial points belonging to inner and outer spheres, respectively. It is convenient to present function (3) as a sum of its spatially averaged part

$$\overline{\varepsilon}=\frac{\varepsilon_{\text{in}}V_{\text{in}}+\varepsilon_{\text{out}}(V_{\text{out}}-V_{\text{in}})}{V_{\text{out}}}\ , \tag{5}$$

with $V_{\text{in/out}}=(4\pi/3)R^3_{\text{in/out}}$ being the volumes of inner and outer spheres, and the summand $\Delta\varepsilon(\mathbf{r})$, the integral of which over the whole resonator volume is equal to zero. The solution to Eq. (1) with exact permittivity value instead of its average one given by (5) will be the starting point to build the constructive perturbation theory.

Equation (1) with coordinate-independent permittivity can be solved by the method described in a number of textbooks (see, e. g., Ref. [18]). The general solution can be presented as an expansion in complete orthogonal eigenfunctions of the Laplace operator, which in spherical coordinates have the form [19,20]

$$|\mathbf{r};\boldsymbol{\mu}\rangle=\frac{D_n^{(l)}}{R}\sqrt{\frac{2}{r}}\,J_{l+\frac{1}{2}}\left(\lambda_n^{(l)}r/R\right)Y_l^m(\vartheta,\varphi) \tag{6}$$

$$\big(n=1,2,\dots,\infty\ ;\quad l=0,1,2,\dots,\infty\ ;\quad m=-l,-l+1,\dots l-1,\ l\big)\ .$$

Here, to simplify the equations we introduce the vector mode index $\boldsymbol{\mu}=\{n,l,m\}$, $J_p(u)$ is the Bessel function of the first kind, $Y_l^m(\vartheta,\varphi)$ is the spherical function,

$$Y_l^m(\vartheta,\varphi)=(-1)^m\left[\frac{(2l+1)}{2}\cdot\frac{(l-m)!}{(l+m)!}\right]^{1/2}P_l^m(\cos\vartheta)\cdot\frac{\mathrm{e}^{im\varphi}}{\sqrt{2\pi}}\ , \tag{7}$$

$P_l^m(t)$ is the Legendre function. The coefficients $\lambda_n^{(l)}$ in the equation (6) are the positive zeros of either the sum $uJ'_{l+\frac{1}{2}}(u)+(1/2)J_{l+\frac{1}{2}}(u)$ (if boundary conditions (BC) (2a) is applied), or the function $J_{l+\frac{1}{2}}(u)$ (in the case of BC (2b)), which are numbered by natural index n in ascending order. Normalization coefficient $D_n^{(l)}$ in relation (6) depends on the particular boundary condition,

$$D_n^{(l)}=\left\{J'^2_{l+\frac{1}{2}}\big(\lambda_n^{(l)}\big)+\left[1-\left(\frac{l+1/2}{\lambda_n^{(l)}}\right)^2\right]J^2_{l+\frac{1}{2}}\big(\lambda_n^{(l)}\big)\right\}^{-\frac{1}{2}}\quad \text{for BC (2a)}, \tag{8a}$$

$$D_n^{(l)}=J^{-1}_{l+\frac{3}{2}}\big(\lambda_n^{(l)}\big)\quad \text{for BC (2b)}. \tag{8b}$$

The eigenvalue of the Laplace operator, that corresponds to eigenfunction (6), is degenerated over azimuthal index m,

$$E_{\boldsymbol{\mu}} = -k_{\boldsymbol{\mu}}^2 = -\left(\frac{\lambda_n^{(l)}}{R}\right)^2 . \tag{9}$$

with the degeneracy equal to $2l+1$.

The spectrum of the resonator with nonuniform permittivity (3) can be found through the calculation of density of states $\nu(k)$ (see, e. g., Ref. [21]). Function $\nu(k)$ can be expressed through the Green function of wave equation (1) with complex-valued frequency account for dissipation in the resonator,

$$\nu(k) = \pi^{-1}\mathrm{Im}\big\{\mathrm{Tr}\,\hat{\mathcal{G}}^{(-)}\big\} . \tag{10}$$

Here $\hat{\mathcal{G}}^{(-)}$ is the advanced Green operator corresponding the equation (1) with negative imaginary part in the complex frequency plane. The Green function (considered as the coordinate matrix element of operator $\hat{\mathcal{G}}^{(-)}$) obeys the equation

$$\big[\varDelta + \overline{\varepsilon}k^2 - i/\tau_d - V(\mathbf{r})\big]\,G(\mathbf{r},\mathbf{r}') = \delta(\mathbf{r}-\mathbf{r}') , \tag{11}$$

where the term $V(\mathbf{r}) = -k^2\varDelta\varepsilon(\mathbf{r})$ will be interpreted as the effective potential (in the quantum-mechanical terminology). In comparison with Eq. (1), equation (11) is supplied with imaginary term i/τ_d which takes phenomenologically into account the dissipation processes in the bulk and on the surface of the resonator. Strictly speaking, the dielectric loss in the resonator depend on the frequency in the general case. Yet now we will neglect this dependence to simplify further investigations.

For the numerical calculation purposes it is suitable to go over from the coordinate representation of Eq. (11) to the momentum representation. Equation (11) then takes the form of an infinite set of coupled algebraic equations,

$$\big(\overline{\varepsilon}k^2 - k_{\boldsymbol{\mu}}^2 - i/\tau_d - \mathcal{V}_{\boldsymbol{\mu}}\big)\,G_{\boldsymbol{\mu}\boldsymbol{\mu}'} - \sum_{\boldsymbol{\nu}\neq\boldsymbol{\mu}}\mathcal{U}_{\boldsymbol{\mu}\boldsymbol{\nu}}G_{\boldsymbol{\nu}\boldsymbol{\mu}'} = \delta_{\boldsymbol{\mu}\boldsymbol{\mu}'} . \tag{12}$$

Here the quantities $\mathcal{V}_{\boldsymbol{\mu}}$ and $\mathcal{U}_{\boldsymbol{\mu}\boldsymbol{\nu}}$, which we will term the *intramode* and the *intermode* potentials, are the matrix elements of potential $V(\mathbf{r})$ taken in the basis of functions (6),

$$\mathcal{U}_{\boldsymbol{\mu}\boldsymbol{\nu}} = \int_{\varOmega} d\mathbf{r}\,\langle\mathbf{r};\boldsymbol{\mu}|\,V(\mathbf{r})\,|\mathbf{r};\boldsymbol{\nu}\rangle = -k^2(\varepsilon_{\mathrm{in}}-\varepsilon_{\mathrm{out}})I_{\boldsymbol{\mu}\boldsymbol{\nu}} , \tag{13a}$$

$$\mathcal{V}_{\boldsymbol{\mu}} = \mathcal{U}_{\boldsymbol{\mu}\boldsymbol{\mu}} = -k^2(\varepsilon_{\mathrm{in}}-\varepsilon_{\mathrm{out}})\big[I_{\boldsymbol{\mu}\boldsymbol{\mu}} - V_{\mathrm{in}}/V_{\mathrm{out}}\big] , \tag{13b}$$

$$I_{\boldsymbol{\mu}\boldsymbol{\nu}} = \int\limits_{\varOmega_{\mathrm{in}}} d\mathbf{r}\langle\mathbf{r};\boldsymbol{\mu}|\mathbf{r};\boldsymbol{\nu}\rangle .$$

In the case of strictly centered outer and inner dielectric spheres the integrals in the relationships (13) are calculated rigorously, and the result is as follows,

$$
\begin{aligned}
I_{\boldsymbol{\mu\nu}}(\Omega_{\text{in}}) =& 2\mathcal{Q}\delta_{l_\mu l_\nu}\delta_{m_\mu m_\nu}\frac{D^{(l_\mu)}_{n_\mu}D^{(l_\mu)}_{n_\nu}}{\lambda^{(l_\mu)2}_{n_\mu}-\lambda^{(l_\mu)2}_{n_\nu}}\Big[\lambda^{(l_\mu)}_{n_\mu}J_{l_\mu+\frac{3}{2}}\left(\lambda^{(l_\mu)}_{n_\mu}\mathcal{Q}\right)J_{l_\mu+\frac{1}{2}}\left(\lambda^{(l_\mu)}_{n_\nu}\mathcal{Q}\right)\\
&-\lambda^{(l_\mu)}_{n_\nu}J_{l_\mu+\frac{1}{2}}\left(\lambda^{(l_\mu)}_{n_\mu}\mathcal{Q}\right)J_{l_\mu+\frac{3}{2}}\left(\lambda^{(l_\mu)}_{n_\nu}\mathcal{Q}\right)\Big] \qquad (\boldsymbol{\mu}\neq\boldsymbol{\nu})\ , \qquad (14a)\\
I_{\boldsymbol{\mu\mu}}(\Omega_{\text{in}}) =& \mathcal{Q}^2\left[D^{(l_\mu)}_{n_\mu}\right]^2\left[J^2_{l_\mu+\frac{1}{2}}\left(\lambda^{(l_\mu)}_{n_\mu}\mathcal{Q}\right)-J_{l_\mu-\frac{1}{2}}\left(\lambda^{(l_\mu)}_{n_\mu}\mathcal{Q}\right)J_{l_\mu+\frac{3}{2}}\left(\lambda^{(l_\mu)}_{n_\mu}\mathcal{Q}\right)\right]. \qquad (14b)
\end{aligned}
$$

Here we have introduced the scale parameter $\mathcal{Q} = R_{\text{in}}/R_{\text{out}} \leqslant 1$ that describes the degree of the resonator *geometric* inhomogeneity.

3 Numerical results and discussion

The set of basic equations (12) can, in principle, be solved analytically using the operator technique of mode separation [14]. Yet, in view of the tediousness of that technique, in this study we examine equations (12) numerically. To obtain the solution we have elaborated programming software that calculate the resonator Green function, determine its maxima locations, and also build the inter-frequency distribution function. It is necessary to accentuate that such a calculation task is quite resource-intensive, and it leads to rigid constraint for the number N of oscillation modes taken into account. The computational complexity grows much faster than N^3. Such a dependence on the number of analyzed oscillations can be explained by the complexity of numerical integration of oscillating functions (Bessel functions, spherical Legendre functions) with the growing number of their zeros on the interval of integration. The main numerical calculations were carried out on the computing cluster at the Institute for Radiophysics and Electronics of National Academy of Sciences of Ukraine, which is a part of the infrastructure of the Ukrainian National Grid (UNG). Based on the available computation resources (CPU clock speed 2.5 GHz, RAM 1.5 Gb/core), we were compelled to limit the number of harmonics by 10,000 and no more than 2000 harmonics for an arbitrary value of heterogeneity. The calculation of each harmonics takes from a few seconds for the long-wavelength modes to tens of minutes for short ones. To speed up the calculations and the possibility to operate with a greater number of harmonics, the parallelization of computational algorithm with the use of MPI technology was implemented. Note that the task under consideration is highly scalable. Thus, the parallel computation provides a performance increase. It is almost proportional to the number of computing nodes involved. All calculations were performed in the standard representation for double-precision real numbers. Relative error of calculation does not exceed 10^6, and the main source of error was the accuracy of numerical integration and calculation of special functions.

From Eqs. (12) we have calculated all diagonal elements of the Green function matrix $\|G_{\boldsymbol{\mu\mu}'}\|$. In Fig. 2, the density of states (DoS) of the resonator is presented, which is calculated using the definition (10). It can be seen that the

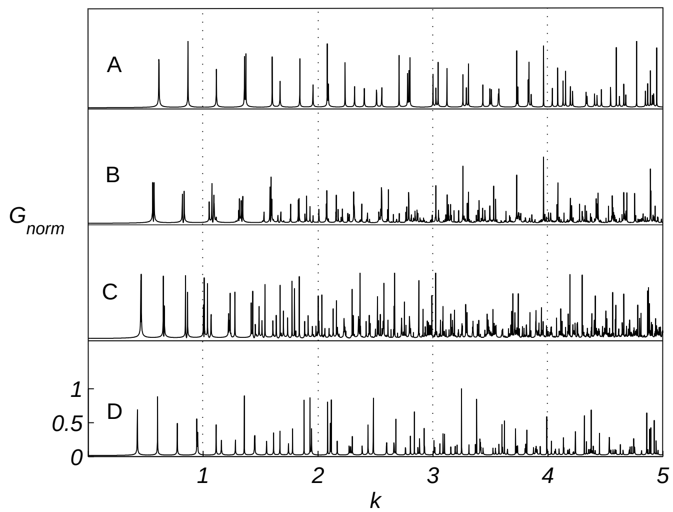

Fig. 2. The whole frequency spectrum as the frequency dependence of the imaginary part of the sum of diagonal Green functions for the composite cavity resonator with centered dielectric spheres: A — $\mathcal{Q}$=0; B — $\mathcal{Q}$=0.583; C — $\mathcal{Q}$=0.897; D — $\mathcal{Q}$=0.998. The permittivities of the inner and outer spheres are $\varepsilon_{\rm in}$= 2.08, $\varepsilon_{\rm out}$ = 1.0. The dissipation value corresponds to τ_d = 1000.

DoS graph becomes thicker with growing the radius of inner dielectric sphere. When the inner radius value goes to the outer one, the DoS is getting thinner. In this case the resonator filling tends to become homogenous with the effective permittivity $\varepsilon_{\rm out}$. Thus, the average DoS maximal value is observed at $\mathcal{Q} \to 1$.

To analyze the oscillation spectrum we examine the probability of the inter-frequency intervals (nearest-neighbor spacings, NNS) between adjacent resonances, $P(S)$. Conventionally, the spectrum unfolding is used for this purpose, implying the normalized mean inter-frequency distance to be equal to unity. Fig. 3 demonstrates distribution $P(S)$ for different inner radii and dissipation values. For τ_d= 100000 (the loss is practically neglected) and $\mathcal{Q}$=0 we have convention with Poisson distribution, $P_p(S) = \exp(-S)$. This suggests the resonance frequencies to be completely uncorrelated. With the increase in the dissipation value (for example, τ_d =100) we obtain the distribution function that tends to Wigner form, $P_w(S) = 0.5\pi S \exp(-\frac{\pi S^2}{4})$. Thus, we are led to conclude that the presence of dissipation in the resonator results in the chaotic behavior of oscillation modes.

The essential difference between NNS distribution of the chaotic spectrum and the regular one is the presence of mode "repulsion" (the downfall of $P(S)$ at low values of S). The repulsion of modes with close frequencies in the chaotic spectrum can be explained as follows. When the resonator infill is homogeneous, different oscillation modes are independent of each other and do not interact with each other even if their own frequencies coincide, i. e. if they are in a degenerate state. Any heterogeneity lifts the degeneracy, and the

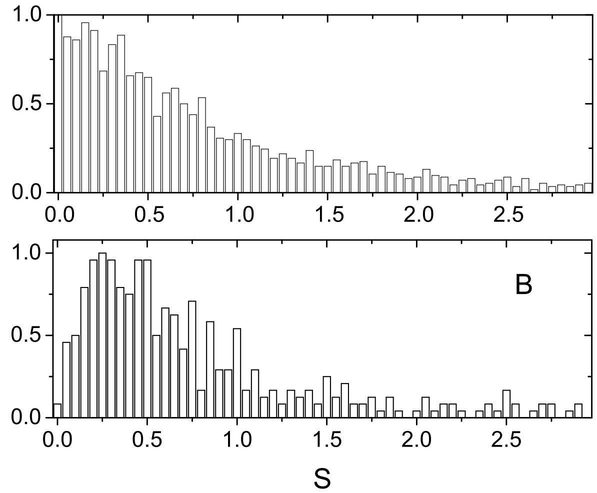

Fig. 3. The probability of inter-frequency interval distribution at different dissipation values and inner radii : A — $\tau_d = 100000$, $\mathcal{Q}$=0; B — $\tau_d = 100$, $\mathcal{Q}$=0.67.

natural frequencies of different modes change in different ways, depending on the degree of heterogeneity influence. That is, there is a kind of "repulsion" of oscillations modes. The larger the impact of heterogeneity be, the greater is the repulsion effect.

In Fig. 4, the intensity of a partial Green function $G_{\boldsymbol{\mu\mu}}$ from Eq. (12) on wave number is shown for the particular polar and radial indices and different inner sphere radii R_{in}. At R_{in}=0 we observe one oscillation mode only. We will call it the main resonance for the selected Green function. With the increase in the inner radius R_{in}, additional resonances appear at the frequencies that coincide with main resonances of the rest of radial modes with the definite polar index.

In Fig. 5, the frequency dependence of the imaginary part of the sum of diagonal Green functions for the oscillations with two different polar indices. As the radius R_{in} increases, we observe that the resonances 1 and 2 interchange their relative position. Thus, we see the occasional and unpredictable oscillations moving. We explain this behavior of resonances as a signature of wave chaos arisen due to inhomogeneity of the resonator.

Thus, we have developed the statistical spectral theory of the centrally symmetric layered cavity resonator with homogeneous and inhomogeneous infill. Numerical investigation of the resonator frequency spectrum was also carried out. The signature of chaotic behavior of the resonator spectrum is demonstrated. We have found out that the homogeneous resonator has inter-frequency interval distribution similar to the Poisson distribution typical for the spectrum with uncorrelated inter-frequency intervals. In the presence of dissipation in

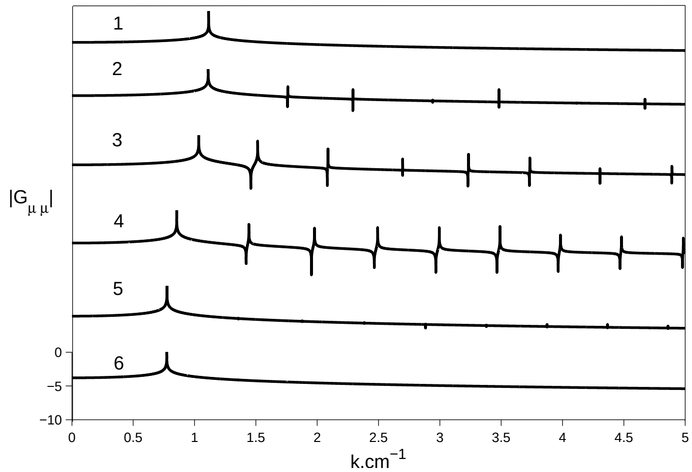

Fig. 4. Frequency dependence of the logarithm of partial normalized Green function for different inner radii: 1 — $\mathcal{Q}$=0, 2 — $\mathcal{Q}$=0.448, 3 — $\mathcal{Q}$=0.672, 4 — $\mathcal{Q}$=0.8968, 5 — $\mathcal{Q}$=0.9977, 6 — $\mathcal{Q}$=0.9997. Polar index is 3, radial index is 1. The permittivities of the inner and outer spheres are $\varepsilon_{\rm in}$=2.08, $\varepsilon_{\rm out}$=1.0. The dissipation value corresponds to $\tau_d = 100000$.

the resonator, the NNS distribution tents to the distribution of Wigner form, which clearly demonstrates the effect of "mode repulsion".

References

1. F. T. Arecchi and R. G. Harrison (eds.). *Instabilities and Chaos in Quantum Optics* (Springer-Verlag, Berlin, 1987).
2. I. O. Kulik and R. Ellialtioglu (eds.). *Quantum mesoscopic phenomena and mesoscopic devices in microelectronics* (Springer Science+Business Media, Dordrecht, 2000).
3. M. C. Gutzwiller. *Resource Letter ICQM-1: The Interplay between Classical and Quantum Mechanics*, Am. J. Phys. **66**, 304 (1998).
4. A. J. Lichtenberg, M. A. Lieberman. *Regular and chaotic dynamics* (Springer-Verlag, New York, 1992).
5. F. Haake. *Quantum Signatures of Chaos* (Springer-Verlag, Berlin, 2010).
6. H.-J. Stöckmann. *Quantum chaos: an introduction* (Cambridge University Press, New York, 1999).
7. V. G. Baryakhtar, V. V. Yanovsky, S. V. Naydenov, and A. V. Kurilo. *Chaos in Composite Billiards*, JETP **103**, 292 (2006).
8. R. Blümel, T. M. Antonsen, B. Georgeot, E. Ott, and R. E. Prange. *Ray Splitting and Quantum Chaos*, **76**, 2476 (1996).
9. R. Blümel, T. M. Antonsen, B. Georgeot, E. Ott, and R. E. Prange. *Ray splitting and quantum chaos*, **53**, 3284 (1996).
10. T. A. Brody, J. Flores, J. B. French, P. A. Mello, A.Pandey, and S. S. M. Wong. *Random-matrix physics: spectrum and strength fluctuations*, **53**, 385 (1981).
11. Yu. V. Tarasov. *Elastic scattering as a cause of quantum dephasing: the conductance of two-dimensional imperfect conductors*, **10**, 395 (2000).

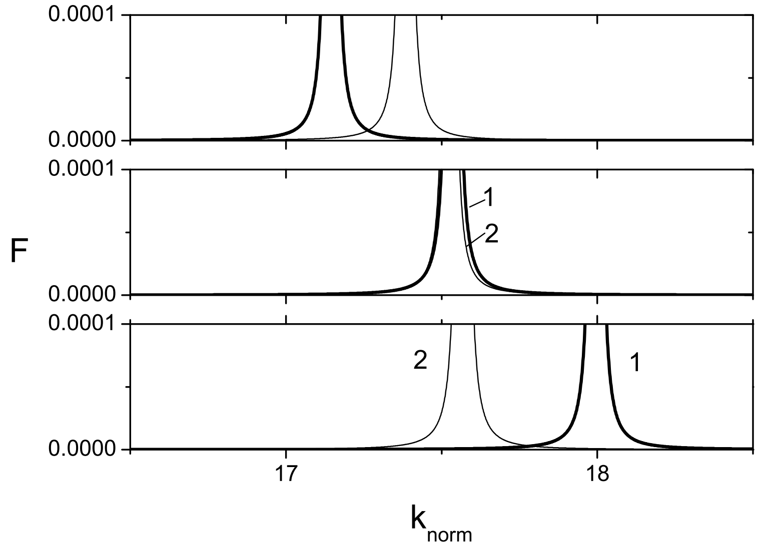

Fig. 5. Frequency dependence of the imaginary part of the sum of diagonal Green functions with fixed polar indices (1 — polar index $l = 1$, 2 — $l = 3$) with different values of radius $R_{\rm in}$: A — $\mathcal{Q}$=0.19, B — $\mathcal{Q}$=0.21, C — $\mathcal{Q}$=0.23. The permittivities of the inner and outer spheres are $\varepsilon_{\rm in}$=2.08, $\varepsilon_{\rm out}$=1.0. The dissipation value corresponds to $\tau_d = 100000$.

12. E. M. Ganapolskii, Z. E. Eremenko, and Yu. V. Tarasov. *Effect of random surface inhomogeneities on spectral properties of dielectric-disk microresonators: Theory and modeling at millimeter wave range*, **79**, 041136 (2009).
13. E. M. Ganapolskii, Yu. V. Tarasov, and L. D. Shostenko. *Spectral properties of cylindrical quasioptical cavity resonator with random inhomogeneous side boundary*, **84**, 026209 (2011).
14. E. M. Ganapolskii, Z. E. Eremenko, and Yu. V. Tarasov. *Influence of random bulk inhomogeneities on quasioptical cavity resonator spectrum*, **75**, 026212 (2007).
15. L. A. Vajnshtejn. *Electromagnetic Waves* (Radio i Svyaz, Moscow, 1988) (in Russian).
16. A. N. Oraevsky. *Whispering-gallery waves*, Quant. Electron. **32**, 377 (2002).
17. K. Gustafson, T. Abe. *The Third Boundary Condition — Was it Robin's?*, Math. Intell. **20**, 63 (1998).
18. A. Messiah. *Quantum Mechanics*, v. 1 (North-Holland, Amsterdam, 1961).
19. G. N. Watson, *A Treatise on the Theory of Bessel Functions* (Cambridge University Press, 1995).
20. H. Bateman, A. Erdélyi, *Higher transcendental functions*, v. 2 (McGraw Hill, New York, 1953).
21. E. N. Economou. *Green's Functions in Quantum Physics* (Springer-Verlag, Berlin, 2006).